

Entanglement Classification for Three-qubit Pure Quantum System using Special Linear Group under the SLOCC Protocol

Amirul Asyraf Zahir¹, Siti Munirah Mohd², Mohd Ilias M Shuhud³, Bahari Idrus⁴, Hishamuddin Zainuddin⁵,
Nurhidaya Mohamad Jan⁶, Mohamed Ridza Wahiddin⁷

Faculty of Science and Technology, Universiti Sains Islam Malaysia, Negeri Sembilan, Malaysia^{1,3}
Kolej PERMATA Insan, Universiti Sains Islam Malaysia, Negeri Sembilan, Malaysia^{2,6}
Center for Artificial Intelligence Technology (CAIT), Faculty of Information Science and Technology,
Universiti Kebangsaan Malaysia, Selangor, Malaysia⁴
1133, Jalan S2 A33, Central Park, Seremban 2, Negeri Sembilan, Malaysia⁵
Tahmidi Centre, Universiti Sains Islam Malaysia, Negeri Sembilan, Malaysia⁷

Abstract—Quantum technology has been introduced in the IR 4.0, breeding a new era of advanced technology revolutionizing the future. Hence, understanding the key resources of quantum technology, quantum entanglement is vital. Growing interests in quantum technologies has raised comprehensive studies of quantum entanglement, especially on the entanglement classification. Special Linear group, $SL(n)$ of multipartite entanglement classification under the SLOCC protocol is not widely studied due to its complex structure, creating a curb in developing its classification method. Therefore, this paper developed and delivered a classification method of pure multipartite, three-qubit quantum state using a combination of Special Linear group, $SL(2) \times SL(2) \times SL(2)$ model operator under the SLOCC, classifying entanglement using the model operator with certain selected parameters. Further analysis was done resulting in the determination of the six subgroups, namely fully separable ($A-B-C$), bi-separable ($A-BC$, $B-AC$ and $C-AB$) and genuinely entangled (W and GHZ).

Keywords—Quantum entanglement; entanglement classification; three-qubit quantum system; special linear group; $SL(2)$; stochastic local operations and classical communication; SLOCC

I. INTRODUCTION

The utilization of quantum entanglement is important in quantum computing, quantum cryptography, and quantum teleportation. This research main focus is the three-qubit quantum system entanglement classification as multipartite entanglement is considered complex and still an open problem [1, 2].

Quantum entanglement is one of the key resources in quantum information processing [3]. An entanglement can be described simply as multiple quantum subsystems states that cannot be described independently, regardless the distances between the subsystems [4]. To put it simply, an object's properties between two or more objects are dependent to each other. Over the years, quantum entanglement has sparked a massive interest of research in numerous fields namely quantum computing, quantum cryptography and quantum teleportation [5-15].

In quantum computing, the utilization of quantum entanglement principles would be a great power fuel [16, 17]. The concept of superposition and quantum bit also known as qubit is the core of a quantum computer. Yu [15] coined, superposition and qubit allows a quantum computer to process information at a significantly higher rate compared to its classical counterpart. It is reported that the most recent achievement made by one of the leader in the game, IBM quantum computer has exceeded over 1000 qubits and the organization has mapped their journey for the next few years [18].

Kumari and Adhikari [19] and Walter, et al. [20] has stated that in multipartite entanglement classification, there exists six inequivalent classes under Stochastic Local Operations and Classical Communication: One fully separable state ($A-B-C$), three bi-separable state ($A-BC$, $B-AC$, $C-AB$), and two genuinely entangled state (W and GHZ). To ensure a successful quantum information processing tasks, entanglement classifications is definitely a must.

In a three-qubit system classification, three main transformation protocols are Local Unitary (LU) protocol, Local Operations and Classical Communication (LOCC) protocol and Stochastic Local Operations and Classical Communication (SLOCC) protocol [21]. In this research, SLOCC protocol is utilized. According to Zha, et al. [22], SLOCC is the key in classifying higher dimensions qubit states and assists in dictating its entanglement within. However, Zha, et al. [22] added along with Lin and Wei [23], the entanglement classification can be challenging with a higher qubit quantum system mainly due to its infinite inequivalent SLOCC classes.

The classification of entanglement under the SLOCC protocol remains a significant challenge in multipartite entanglement. This event is still not well understood and rather complicated to be generally analysed [3, 20-22, 24-26]. Consequently, any transformed quantum state cannot be observed to execute the similar quantum information processing tasks [24].

The purpose of classifying entanglement under the SLOCC is to class the quantum states respectively to its tasks [21, 27, 28]. Two states $|\psi\rangle$ and $|\phi\rangle$ are SLOCC equivalent if both can execute a similar quantum information processing tasks [22]. According to M. Cunha, et al. [29], pure three-qubit GHZ and W states are non-equivalent under SLOCC. It means that it is unfeasible to transform a class state into another class state conversely. Li, et al. [30] stated SLOCC holds an advantage over LOCC that is SLOCC take on an uncomplicated mathematical form.

Research on a different group and protocol, namely Special Unitary group, $SU(n)$ under Local Unitary (LU) protocol has been conducted to unfold the issue in multipartite state transformation. Nevertheless, the classification of multipartite entanglement in Special Linear group, $SL(n)$ has its limitation in determining the particular quantum state classes as a consequence of the complexity of multipartite concept under SLOCC protocol [20, 31, 32]. Reason for this complication is that there are infinite number of SLOCC classes and the overlapping Special Linear group, $SL(n)$ subgroups [20, 31].

The main purpose of this research is to develop a straightforward multipartite entanglement classification model under the SLOCC protocol. This study employed Von Neumann entropy measurement, $S(\rho_i) = -\text{Tr}(\rho_i \ln \rho_i)$, $i = A, B, C$, specifically to detect an entanglement of the quantum states. The paper is organized as follows. The research methodology is detailed in Section II, followed by results and discussion in Section III and Section IV concludes the research.

II. METHODOLOGY

The modeling process of the $SL(2) \times SL(2) \times SL(2)$ operator model included the following steps:

- 1) Understanding the measurement for $SL(2)$ parameterization. The variables of both the generator and parameters were thoroughly investigated at this stage.
- 2) Aligning the selected parameters with the used generator. This step established the parameter range to be used.
- 3) Developing the matrix for the operator model and implementing it in Mathematica 13.2.
- 4) The $SL(2) \times SL(2) \times SL(2)$ operator model full development. The process starts with combining the developed operator model with the initial pure quantum states to create a three-qubit quantum system.

Mathematica 13.2 software was chosen for its symbolic and numerical computations processing capabilities, making it suitable for simulations and mathematical modeling. It offers a powerful platform for creating and manipulating mathematical expressions and formulations, which is crucial for the development of the $SL(2) \times SL(2) \times SL(2)$ operator model.

Three parameters were selected and incorporated into the $SL(2) \times SL(2) \times SL(2)$ operator model because they have a significant influence on the correlated qubits:

- 1) The translation parameter w was represented within the range of $-\infty \rightarrow +\infty$, illustrating the position of a particle, which can take both positive and negative values.
- 2) The scaling parameter r was represented within the range of $0 \rightarrow +\infty$, illustrating the size of a particle, which can only take a positive value.
- 3) The rotation parameter t was represented within the range of $0 \rightarrow 2\pi$, illustrating the precise position of a particle within a plane.

The specific parameter values selected for every initial pure quantum state system are presented in the results section. Both operator model, $SL(2)$ and $SL(2) \times SL(2) \times SL(2)$ was developed in Mathematica 13.2. Fig. 1 shows the steps in developing the matrix for $SL(2) \times SL(2) \times SL(2)$ operator model.

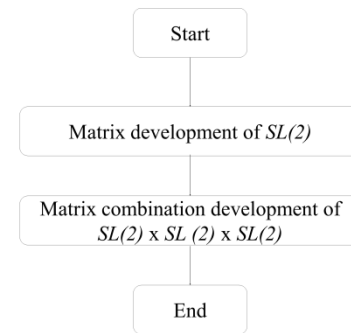


Fig. 1. $SL(2) \times SL(2) \times SL(2)$ operator model matrix development.

The development of the $SL(2)$ operator model began with the representation of $SL(2)$ as series expansions of exponential, cosine, and sine functions. The mathematical model was extended after completing the matrix development of the initial $SL(2)$ operator model. The $SL(2) \times SL(2) \times SL(2)$ model is designed to represent a multi-qubit quantum system, as the initial $SL(2)$ operator model only accounted for a single-qubit quantum system. The tensor product of $SL(2) \times SL(2) \times SL(2)$ operator model resulted in a large 8×8 composite matrix. Illustrated in Fig. 3 is the operator model for $SL(2) \times SL(2) \times SL(2)$. The $SL(2) \times SL(2) \times SL(2)$ operator model is denoted as $SL2$ from this point onward. The development went through several critical steps for its completion as illustrated in Fig. 2.

Fig. 2 shows the $SL2$ operator model in action on a fully separable quantum state, resulting in $SL2|000\rangle$. In this study, the $SL2$ operator model is also applied to bi-separable ($A-BC$) and genuinely entangled (W and GHZ) quantum states. The combination procedure of $SL2$ is illustrated in Fig. 4.

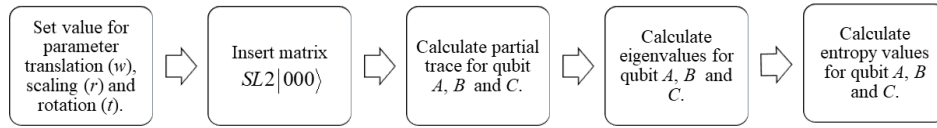


Fig. 2. SL(2) x SL(2) x SL(2) operator model development.

$$SL(2) = \begin{pmatrix} 2.718282 (\cos [b1]) - i \sin [b1] & 0.3678794 (\cos [b1]) - i \sin [b1] \\ 0 & 0.3678794 (\cos [b1]) - i \sin [b1] \end{pmatrix}$$

$$SL(2) \otimes SL(2) \otimes SL(2) = \begin{pmatrix} 20.08554 (\cos [b1] - i \sin [b1])^3 & \dots & \dots & \dots & \dots & \dots & \dots & 0.049787 (\cos [b1] - i \sin [b1])^3 \\ 0 & \dots & \dots & \dots & \dots & \dots & \dots & 0.049787 (\cos [b1] - i \sin [b1])^2 (\cos [b1] + i \sin [b1]) \\ 0 & \dots & \dots & \dots & \dots & \dots & \dots & 0.049787 (\cos [b1] - i \sin [b1])^2 (\cos [b1] + i \sin [b1]) \\ 0 & \dots & \dots & \dots & \dots & \dots & \dots & 0.049787 (\cos [b1] - i \sin [b1]) (\cos [b1] + i \sin [b1])^2 \\ 0 & \dots & \dots & \dots & \dots & \dots & \dots & 0.049787 (\cos [b1] - i \sin [b1])^2 (\cos [b1] + i \sin [b1]) \\ 0 & \dots & \dots & \dots & \dots & \dots & \dots & 0.049787 (\cos [b1] - i \sin [b1]) (\cos [b1] + i \sin [b1])^2 \\ 0 & \dots & \dots & \dots & \dots & \dots & \dots & 0.049787 (\cos [b1] - i \sin [b1]) (\cos [b1] + i \sin [b1])^2 \\ 0 & \dots & \dots & \dots & \dots & \dots & \dots & 0.049787 (\cos [b1] + i \sin [b1])^3 \end{pmatrix}$$

Fig. 3. SL(2) x SL(2) x SL(2) operator model.

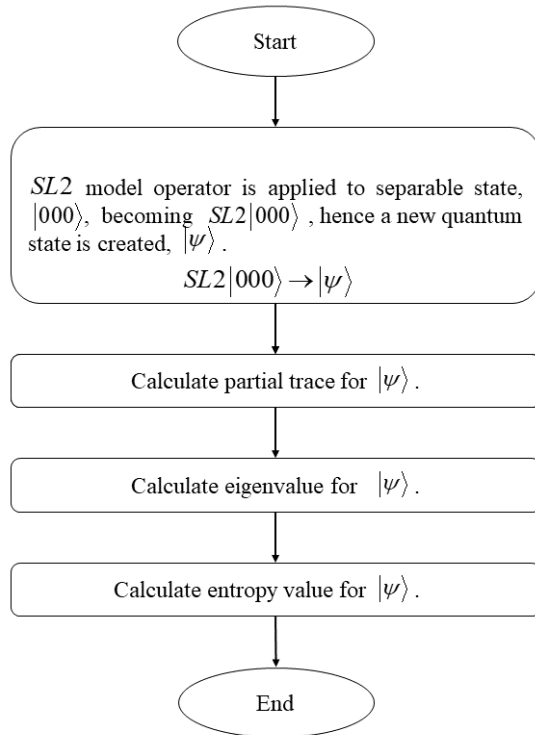


Fig. 4. SL 2 operator model combination procedure.

III. RESULTS AND DISCUSSION

As shown in Fig. 4, the *SL2* operator model is applied to a fully separable quantum state, resulting in a new combined quantum state denoted as $|\psi\rangle$. It was also applied to bi-separable ($A-BC$) as well as genuinely entangled (W and GHZ) quantum states. Each quantum state was simulated using two sets of translation and scaling values, each of which contained 24 rotation values. The simulations provide valuable insights into the characteristics of the quantum states when acted upon by the operator model under various values of translation, scaling, and rotation.

The translation parameter was selected within the range of $-\infty \rightarrow +\infty$ while the scaling parameter is selected within the range of $0 \rightarrow +\infty$. The rotation angle parameters were determined and selected within $0 \rightarrow 2\pi$, which encompassed all four quadrants of the Cartesian plane. There are two main case simulations: Case 1 and Case 2. In each case, the translation and scaling values were fixed while different rotation angles were used. Table I shows the values used for translation and scaling, while Table II shows the values used for rotation.

TABLE I. TRANSLATION (w) AND SCALING (r) PARAMETERS

Case	Parameters
1	$w = 1, r = 1$
2	$w = -1, r = \frac{1}{2}$

The classification process was influenced by the values of all three parameters, as listed in Table I and II. The von Neumann entropy is given by $S(\rho_i) = -\text{Tr}(\rho_i \ln \rho_i)$, $i = A, B, C$. The value of this entropy range between $0 \leq S(r) \leq 1$ for all density matrix r , with 0 indicating a fully separable quantum state and 1 indicating the maximum value of entanglement. These values enable us to observe the degree of entanglement for specific quantum states and further classify them based on the parameter combinations used in each simulation.

The simulation's initial quantum states cover four out of six entanglement classes under the SLOCC protocol: fully separable ($A-B-C$), bi-separable ($A-BC$, $B-AC$, $C-AB$), and genuinely entangled (W and GHZ). The other two classes of bi-separable ($B-AC$ and $C-AB$) were not considered separately because their attributes are similar and can be represented by the $A-BC$ class. The combination of these initial quantum states with the operator model generated a new quantum state, representing the combination after the transformation. The new quantum state was then acted upon by three selected parameters: translation, scaling, and rotation.

Table III summarizes the classification of pure three-qubit entanglement simulations for fully separable, bi-separable, and genuinely entangled states using a special linear group under the SLOCC protocol and the von Neumann entropy measurement. The study successfully classified pure three-

qubit entanglement of the initial quantum states as fully separable, bi-separable, and genuinely entangled. The simulations revealed that the final quantum state remained unchanged from the initial quantum state in some cases, while the parameter selection manipulation changed the final quantum state in others. The simulation results demonstrated that the entanglement class of a quantum state can be altered or maintained by controlling the translation, scaling, and rotation parameters while adhering to the SLOCC protocol. This demonstrates the significance of these parameters in influencing the entanglement properties of a quantum system.

TABLE II. ROTATION (r) PARAMETERS

Quadrant	Angle (π)	Angle ($^\circ$)
1 st	$\frac{\pi}{2}$	90
	$\frac{\pi}{4}$	45
	$\frac{\pi}{6}$	30
	$\frac{\pi}{8}$	22.5
	$\frac{\pi}{10}$	18
	$\frac{\pi}{12}$	15
2 nd	π	180
	$\frac{3\pi}{4}$	135
	$\frac{5\pi}{6}$	150
	$\frac{7\pi}{8}$	157.5
	$\frac{9\pi}{10}$	162
	$\frac{11\pi}{12}$	165
3 rd	$\frac{3\pi}{2}$	270
	$\frac{5\pi}{4}$	225
	$\frac{7\pi}{6}$	210
	$\frac{9\pi}{8}$	202.5
	$\frac{11\pi}{10}$	198
	$\frac{13\pi}{12}$	195
4 th	2π	360
	$\frac{7\pi}{4}$	315
	$\frac{11\pi}{6}$	330
	$\frac{15\pi}{8}$	337.5
	$\frac{19\pi}{10}$	342
	$\frac{23\pi}{12}$	345

TABLE III. PURE THREE-QUBIT ENTANGLEMENT CLASSIFICATION

Initial Quantum State	Case	Rotation (t)	Final Quantum State
A-B-C	1	$\frac{\pi}{2}, \frac{\pi}{4}, \frac{\pi}{6}, \pi, \frac{5\pi}{6}, \frac{7\pi}{8}, \frac{9\pi}{10}, \frac{11\pi}{12}, \frac{3\pi}{2}, \frac{7\pi}{6}, \frac{9\pi}{8}, \frac{11\pi}{10}, \frac{13\pi}{12}, \frac{7\pi}{4}, \frac{11\pi}{6}$	A-B-C
	2	$\frac{\pi}{2}, \frac{\pi}{4}, \frac{\pi}{6}, \pi, \frac{5\pi}{6}, \frac{7\pi}{8}, \frac{9\pi}{10}, \frac{11\pi}{12}, \frac{3\pi}{2}, \frac{7\pi}{6}, \frac{9\pi}{8}, \frac{11\pi}{10}, \frac{13\pi}{12}, \frac{7\pi}{4}, \frac{11\pi}{6}$	
A-BC	1	$\frac{\pi}{2}, \frac{\pi}{4}, \frac{5\pi}{6}, \frac{7\pi}{8}, \frac{9\pi}{10}, \frac{11\pi}{12}, \frac{3\pi}{2}, \frac{7\pi}{6}, \frac{9\pi}{8}, \frac{11\pi}{10}, \frac{13\pi}{12}$	A-B-C
		$\frac{7\pi}{4}$	A-BC
	2	$\frac{\pi}{2}, \frac{3\pi}{4}, \frac{5\pi}{6}, \frac{3\pi}{2}, \frac{5\pi}{4}, \frac{7\pi}{6}$	A-B-C
		$\frac{\pi}{10}, \frac{\pi}{12}, \frac{7\pi}{8}, \frac{9\pi}{8}, 2\pi, \frac{15\pi}{8}, \frac{19\pi}{10}, \frac{23\pi}{12}$	A-BC
W	1	$\frac{\pi}{2}, \pi, \frac{3\pi}{4}, \frac{5\pi}{6}, \frac{7\pi}{8}, \frac{9\pi}{10}, \frac{11\pi}{12}, \frac{3\pi}{2}, \frac{5\pi}{4}, \frac{7\pi}{6}, \frac{9\pi}{8}, \frac{11\pi}{10}, \frac{13\pi}{12}$	A-BC
		$\frac{\pi}{2}, \pi, \frac{3\pi}{4}, \frac{5\pi}{6}, \frac{7\pi}{8}, \frac{9\pi}{10}, \frac{11\pi}{12}, \frac{3\pi}{2}, \frac{5\pi}{4}, \frac{7\pi}{6}, \frac{9\pi}{8}, \frac{11\pi}{10}, \frac{13\pi}{12}$	A-B-C
	2	$\frac{\pi}{4}, \frac{\pi}{6}, \frac{\pi}{8}, \frac{\pi}{10}, \frac{\pi}{12}, 2\pi, \frac{7\pi}{4}, \frac{11\pi}{6}, \frac{15\pi}{8}, \frac{19\pi}{10}, \frac{23\pi}{12}$	GE
		$\frac{\pi}{4}, \pi, \frac{7\pi}{8}, \frac{9\pi}{10}, \frac{11\pi}{12}, \frac{9\pi}{8}, \frac{11\pi}{10}, \frac{13\pi}{12}, \frac{7\pi}{4}$	A-B-C
GHZ	1	$\frac{\pi}{4}, \pi, \frac{7\pi}{8}, \frac{9\pi}{10}, \frac{11\pi}{12}, \frac{9\pi}{8}, \frac{11\pi}{10}, \frac{13\pi}{12}, \frac{7\pi}{4}$	A-B-C
		$\frac{\pi}{6}, \frac{7\pi}{6}$	GE
	2	$\frac{\pi}{2}, \frac{\pi}{4}, \frac{\pi}{6}, \pi, \frac{5\pi}{6}, \frac{7\pi}{8}, \frac{9\pi}{10}, \frac{11\pi}{12}, \frac{3\pi}{2}, \frac{7\pi}{6}, \frac{9\pi}{8}, \frac{11\pi}{10}, \frac{13\pi}{12}, \frac{7\pi}{4}, \frac{11\pi}{6}$	A-B-C
		$\frac{\pi}{8}, \frac{15\pi}{8}$	GE

IV. CONCLUSION

This study focused on the entanglement classification of the pure three-qubit quantum system using a novel mathematical operator model $SL2$ based on the special linear group principles under the SLOCC protocol. The $SL2$ operator model derived was successfully developed using Mathematica.

The utilization of special linear group definitely has its advantage over special unitary group, as it can principally increase and decrease the degree of entanglement of the quantum systems, while special unitary group maintains the entanglement of quantum states. The simulations resulted in the entanglement classification of the three-qubit quantum system into fully separable ($A-B-C$), bi-separable ($A-BC$), and genuinely entangled (GE) states, which were validated with previous studies to demonstrate the success of the developed operator model.

Additionally, the operator model has the potential to be extended to entanglement classification for mixed quantum states for three-qubit quantum systems. Valuable conclusions

about the effects of parameter manipulation on entanglement states can be drawn, contributing to a better understanding of quantum entanglement and its potential applications in quantum information processing.

ACKNOWLEDGMENT

This research is part of a research project supported by the Malaysian Ministry of Higher Education Fundamental Research Grant Nos. FRGS/1/2021/ICT04/USIM/01/1 (USIM/FRGS/KGI/KPT/50121).

REFERENCES

- [1] Sun, Yize, Lin Chen, and Li-Jun Zhao. "Tripartite genuinely entangled states from entanglement-breaking subspaces". Journal of Physics A: Mathematical and Theoretical, 54 No. 2 (2020): p. 025303 <https://doi.org/10.1088/1751-8121/abc20>.
- [2] Wu, Qi-Feng. "Entanglement Classification via Operator Size: a Monoid Isomorphism". arXiv preprint arXiv:2111.07636, No. (2022): p.
- [3] Jaffali, Hamza, and Frédéric Holweck. "Quantum entanglement involved in Grover's and Shor's algorithms: the four-qubit case". Quantum Information Processing, 18 No. 5 (2019): p. 133 <https://doi.org/10.1007/s11128-019-2249-y>.

- [4] Guo, Yuying. "Introduction to quantum entanglement". AIP Conference Proceedings, 2066 No. 1 (2019): p. 020009 <https://doi.org/10.1063/1.5089051>.
- [5] Kirsanov, N. S., V. A. Pastushenko, A. D. Kodukhov, M. V. Yarovikov, A. B. Sagingalieva, D. A. Kronberg, M. Pflitsch, and V. M. Vinokur. "Forty thousand kilometers under quantum protection". Scientific Reports, 13 No. 1 (2023): p. 8756 <https://doi.org/10.1038/s41598-023-35579-6>.
- [6] Erkiş, Ö. L. Conlon, B. Shajilal, S. Kish, S. Tserkis, Y. S. Kim, P. K. Lam, and S. M. Assad. "Surpassing the repeaterless bound with a photon-number encoded measurement-device-independent quantum key distribution protocol". npj Quantum Information, 9 No. 1 (2023): p. <https://doi.org/10.1038/s41534-023-00698-5>.
- [7] Chen, Z., X. Wang, S. Yu, Z. Li, and H. Guo. "Continuous-mode quantum key distribution with digital signal processing". npj Quantum Information, 9 No. 1 (2023): p. <https://doi.org/10.1038/s41534-023-00695-8>.
- [8] Perepechaenko, M., and R. Kuang. "Quantum encryption of superposition states with quantum permutation pad in IBM quantum computers". EPJ Quantum Technology, 10 No. 1 (2023): p. <https://doi.org/10.1140/epjqt/s40507-023-00164-3>.
- [9] Andronikos, Theodore, and Alla Sirokofskich. "An Entanglement-Based Protocol for Simultaneous Reciprocal Information Exchange between 2 Players". Electronics, 12 No. 11 (2023): p. 2506 <https://doi.org/https://doi.org/10.3390/electronics12112506>.
- [10] Li, Zhenghua, Xiangyu Wang, Ziyang Chen, Tao Shen, Song Yu, and Hong Guo. "Impact of non-orthogonal measurement in Bell detection on continuous-variable measurement-device-independent quantum key distribution". Quantum Information Processing, 22 No. 6 (2023): p. 236 <https://doi.org/10.1007/s11128-023-03993-4>.
- [11] Li, Fulin, Tingyan Chen, and Shixin Zhu. "A (t, n) Threshold Quantum Secret Sharing Scheme with Fairness". International Journal of Theoretical Physics, 62 No. 6 (2023): p. 119 <https://doi.org/10.1007/s10773-023-05383-z>.
- [12] Tan, Yongjian, Liang Zhang, Tianxing Sun, Zhihua Song, Jincai Wu, and Zhiping He. "Polarization compensation method based on the wave plate group in phase mismatch for free-space quantum key distribution". EPJ Quantum Technology, 10 No. 1 (2023): p. 6 <https://doi.org/10.1140/epjqt/s40507-023-00163-4>.
- [13] Shen, Si, Chenzhi Yuan, Zichang Zhang, Hao Yu, Ruiming Zhang, Chuanrong Yang, Hao Li, Zhen Wang, You Wang, Guangwei Deng, Haizhi Song, Lixing You, Yunru Fan, Guangcan Guo, and Qiang Zhou. "Hertz-rate metropolitan quantum teleportation". Light: Science & Applications, 12 No. 1 (2023): p. 115 <https://doi.org/10.1038/s41377-023-01158-7>.
- [14] Haddadi, Saeed, and Mohammad Bohloul. "A Brief Overview of Bipartite and Multipartite Entanglement Measures". International Journal of Theoretical Physics, 57 No. (2018): p. 3912–16 <https://doi.org/10.1007/s10773-018-3903-3>.
- [15] Yu, Yue. "Advancements in Applications of Quantum Entanglement". Journal of Physics: Conference Series, 2012 No. 1 (2021): p. 012113 <https://doi.org/10.1088/1742-6596/2012/1/012113>.
- [16] Pan, Jie. "Characterizing true quantum computing power". Nature Computational Science, 1 No. 1 (2021): p. 15-15 <https://doi.org/10.1038/s43588-020-00018-3>.
- [17] Asif, Naema, Uman Khalid, Awais Khan, Trung Q. Duong, and Hyundong Shin. "Entanglement detection with artificial neural networks". Scientific Reports, 13 No. 1 (2023): p. 1562 <https://doi.org/10.1038/s41598-023-28745-3>.
- [18] "The IBM Quantum Development Roadmap." 2023, <https://www.ibm.com/quantum/roadmap>.
- [19] Kumari, Anu, and Satyabrata Adhikari. "Classification witness operator for the classification of different subclasses of three-qubit GHZ class". Quantum Information Processing, 20 No. 9 (2021): p. 316 <https://doi.org/10.1007/s11128-021-03250-6>.
- [20] Walter, Michael, David Gross, and Jens Eisert. "Multi-partite entanglement". No. (2017): p.
- [21] Li, Dafa. "Stochastic local operations and classical communication (SLOCC) and local unitary operations (LU) classifications of n qubits via ranks and singular values of the spin-flipping matrices". Quantum Information Processing, 17 No. (2018): p. <https://doi.org/10.1007/s11128-018-1900-3>.
- [22] Zha, Xinwei, Irfan Ahmed, Da Zhang, Wen Feng, and Yanpeng Zhang. "Stochastic local operations and classical communication invariants via square matrix". Laser Physics, 29 No. (2019): p. 025203 <https://doi.org/10.1088/1555-6611/aaf637>.
- [23] Lin, Lijunzhi, and Zhaohui Wei. "Testing multipartite entanglement with Hardy's nonlocality". Physical Review A, 101 No. 5 (2020): p. 052118 <https://doi.org/10.1103/PhysRevA.101.052118>.
- [24] Li, Dafa. "SLOCC classification of n qubits invoking the proportional relationships for spectrums and standard Jordan normal forms". Quantum Information Processing, 17 No. 1 (2017): p. 1 <https://doi.org/10.1007/s11128-017-1770-0>.
- [25] Aulbach, Martin. "Symmetric entanglement classes for n qubits". arXiv preprint arXiv:1103.0271, No. (2011): p.
- [26] Dietrich, Heiko, Willem A De Graaf, Alessio Marrani, and Marcos Origlia. "Classification of four qubit states and their stabilisers under SLOCC operations". Journal of Physics A: Mathematical and Theoretical, No. (2022): p. <https://doi.org/https://doi.org/10.1088/1751-8121/ac4b13>.
- [27] Backens, Miriam. "Number of superclasses of four-qubit entangled states under the inductive entanglement classification". Physical Review A, 95 No. 2 (2017): p. 022329 <https://doi.org/10.1103/PhysRevA.95.022329>.
- [28] Kumari, Anu, and Satyabrata Adhikari. "Classification witness operator for the classification of different subclasses of three-qubit GHZ class". Quantum Information Processing, 20 No. (2021): p. <https://doi.org/10.1007/s11128-021-03250-6>.
- [29] M. Cunha, Márcio, Alejandro Fonseca, and Edilberto O. Silva. "Tripartite Entanglement: Foundations and Applications". Universe, 5 No. 10 (2019): p. 209
- [30] Li, Yinan, Youming Qiao, Xin Wang, and Runyao Duan. "Tripartite-to-Bipartite Entanglement Transformation by Stochastic Local Operations and Classical Communication and the Structure of Matrix Spaces". Communications in Mathematical Physics, 358 No. 2 (2018): p. 791-814 <https://doi.org/10.1007/s00220-017-3077-5>.
- [31] Gharahi, Masoud, Stefano Mancini, and Giorgio Ottaviani. "Fine-structure classification of multiqubit entanglement by algebraic geometry". Physical Review Research, 2 No. 4 (2020): p. 043003 <https://doi.org/10.1103/PhysRevResearch.2.043003>.
- [32] Burchardt, Adam, and Zahra Raissi. "Stochastic local operations with classical communication of absolutely maximally entangled states". Physical Review A, 102 No. (2020): p.